CHAPTER 5
SIMULATION OF A PAYLOAD FAIRING

In the preceding chapters, a model of a PZT actuator exciting a SS cylinder has been presented. The structural model is based on a modal expansion formulation and is used to compute the internal acoustic response of a cylinder using the Kirchoff-Helmholtz integral and a boundary element formulation. Verification of the structural model was presented in Chapter 2 while the numerical acoustic model was validated analytically in Chapter 3 and experimentally in Chapter 4. In this chapter the overall model is used to predict the internal acoustic response of a large scale SS cylinder which emulates a rocket payload fairing excited by PZT actuators. The acoustic authority and electrical current requirements of the actuator are addressed.

5.1 Properties of the Payload Fairing

The payload fairing that is being considered is the "Minotaur" fairing, currently being manufactured by Boeing corporation. The approximate fairing dimensions are shown in Fig. 5.1. The fairing wall is constructed of an advanced-grid-stiffened (AGS) composite material (Newbury, et al., 1998). The properties of the composite material can be found in Table 5.1 (Griffin, 1999). The AGS material is designed to be lightweight and stiff. For an aluminum plate having a uniform thickness, the plate would only be 1.06×10^{-3} m thick, if it was to have an equivalent area density.

5.2 Choice of Parameters for a Large Scale SS Cylinder

In order for a large scale cylinder to emulate the dynamical properties of a Minotaur payload fairing, several factors must be considered. These factors include cylinder size, stiffness, mass density, damping, and modal frequency location. The parameters of the actuator also need to be addressed with respect to size, location, applied voltage, electro-mechanical properties, etc. The acoustic field varies within the cylinder from place to place, and some locations are more representative of the field as a whole than others. The purpose of this section is to address these issues and indicate the selection of the various parameters used in this analysis.

5.2.1 Cylinder Size

The length and diameter of the cylinder are chosen based on the dimensions of the Minotaur fairing, described in Fig. 5.1. Since the cylinder and the fairing have different geometry, a rigorous scaling analysis is difficult and beyond the scope of this work. The choice of cylinder length and diameter are chosen to be 4.311 m and 1.552 m, respectively. A cross section of the chosen cylinder compared to the Minotaur fairing is shown in Fig. 5.1. These values are selected such that the fairing and the cylinder have the same diameter and similar length.

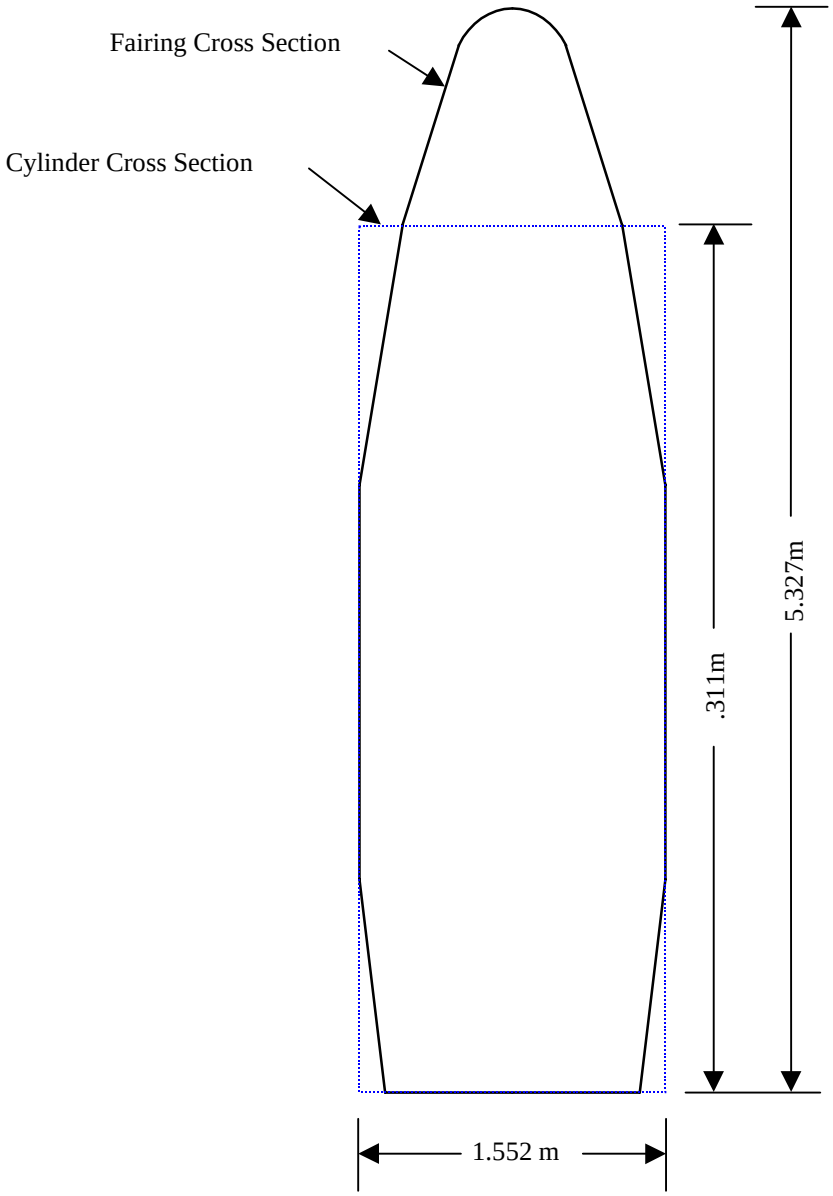

Figure 5.1 Minotaur fairing approximate dimensions and modeled cylinder section.

Table 5.1 Mechanical properties of AGS composite material

Property	Value
Young's Modulus, along fiber (GPa; psi)	171.7; $25x10^6$
Young's Modulus, across fiber (GPa; psi)	10.09; $1.47x10^6$
Shear Modulus (GPa; psi)	6.25; $0.91x10^6$
Poisson's Ratio	0.3
Ply Thickness (m; in.)	$1.27x10^{-4}$; 0.005
Area Density (kg/m^2)	2.86
Skin Thickness (m; in.)	$1.016x10^{-3}$; 0.040

5.2.2 Cylinder Mass and Stiffness

The stiffness of a uniform cylinder is determined by the thickness of the shell, the modulus of elasticity and Poisson's ratio for the material used. The fairing is made of an advanced-grid-stiffened composite material which has a bending stiffness to weight ratio that is higher than any existing material having uniform distribution. Since it is necessary to match the dynamical properties of the uniform cylinder to the fairing, the properties of the AGS composite need to be "smeared". However, information on the dynamic smearing of grid structures in the literature is extremely limited (White and Gilliam, 1983).

Several dynamical properties of the fairing are known and can be used to tailor a model for a cylinder which emulates an actual payload fairing. One of these properties is the area density of the AGS composite material. For all of the test cases in this analysis, the area density is chosen to match that of the Minotaur fairing (2.86 kg/m^2). Therefore, once the cylinder thickness is determined, the material mass density is artificially adjusted, until the area density matches that of the fairing. The other dynamic property of the fairing that is known, is the first shell mode frequency. For the STARS payload fairing (similar in size to the Minotaur fairing), the first shell mode occurs at approximately 75 Hz (Glaese and Anderson, 1999). For all of the test cases in this analysis, the stiffness of the fairing is adjusted until the first shell mode occurs at 75 Hz.

Since the material modulus of elasticity and cylinder thickness determine the stiffness of the cylinder, these properties need to be chosen to match the dynamic properties of the cylinder to the fairing. The modulus of elasticity of the AGS composite material ranges from 10.09 to 171.7 GPa, depending on the fiber orientation (69 GPa for Aluminum). Each ply of the fibers are oriented orthogonally within the AGS fairing skin. This implies that the overall modulus of elasticity of the composite ranges between the two extreme values. Based on this assumption, it is possible to identify the equivalent cylinder thickness and mass density if the modulus of elasticity is assumed and the area mass density and first shell mode frequency are known.

Since the equivalent modulus of elasticity of the fairing material is not known exactly, the analysis is performed for seven cases (50.9, 70.9, 90.9, 110.9, 130.9, 150.9, and 170.9 GPa; cases 1-7, respectively). Case 2 represents a modulus similar to aluminum while case 3 represents the average value of the two extreme moduli for the Minotaur fairing. Once a modulus is chosen for a particular case, the remaining properties (thickness and volumetric mass density) are adjusted such that the first shell mode frequency is 75 Hz and the area mass density is 2.86$kg.m^2$. The cylinder properties for the various cases are shown in Table 5.2. The structural modal frequencies of the cylinder can be found in Appendix F. Unless otherwise noted, Poisson's ratio is assumed to be 0.3.

5.2.3 Cylinder Damping

Damping in an AGS composite plate has also been investigated. It was found that the damping ranged from 0.35 to 2.6 (% of critical) with a mean value of 1.03 (Newbury, et al., 1998). This implies that the structural loss factor (hysteretic damping) ranges from 0.007 to 0.052 with a mean value of 0.0206, at the resonant frequencies (Nashif, 1985). In this analysis the damping for the seven different cases (described in section 5.2.2) are also repeated for three different

values of structural damping (loss factor = 0.007, 0.206 and 0.052). In all of the simulations an acoustic loss factor of 0.001 is used. This is the value that is obtained experimentally as described in chapter 4.

Table 5.2 Physical properties of an equivalent cylinder

Property	Case 1	Case 2	Case 3	Case 4	Case 5	Case 6	Case 7
Thickness (mm)	5.58	4.78	4.30	3.93	3.64	3.39	3.19
Modulus (GPa)	50.9	70.9	90.9	110.9	130.9	150.9	170.9
Density (kg/m^3)	512.5	597.8	665.1	727.7	785.7	843.7	896.6

5.2.4 Baseline PZT Actuator: Material and Physical Properties

The PZT actuator material chosen in this analysis is PSI-5H-S2 (Piezo Systems, Inc.). This particular material is chosen because of its high electromechanical coupling. The electrical properties of this material are found in Table 5.3. The maximum electric field that can be safely applied to a PZT, to prevent depoling of the actuator, is a material property. The maximum field and the thickness of the actuator determine the maximum allowable applied voltage. Because the actuator is intended to be embedded within the fairing skin, its thickness is limited by the thickness of the fairing skin (1.016 mm; 0.04 in.). Each of the composite plies within the skin is approximately 0.127 mm (0.005 in.) thick and can be assumed to cover the actuator. Therefore, the actuator thickness chosen to be modeled in this analysis is 0.762 mm (0.030 in.). Because the impedance model is based on two colocated actuators, two PZT actuators each having a thickness of 0.381 mm (0.015 in.), driven at half the voltage, produce an equivalent structural response. Because the thickness and the depolarization field (electric field = 300 kV/m) determine the maximum applied voltage, the voltage applied to each of the colocated actuators in this analysis is 114.3V (80.82 Vrms). This is equivalent to a single actuator embedded at the neutral axis, with an applied voltage of 228.6 V (161.64 Vrms). If the applied voltage exceeds this level, the PZT actuators will begin to depole and their performance will be compromised.

The actuator size is chosen such that it is small enough to couple well with the significant lower order structural modes. The actuator length is chosen to be 5% of the cylinder length (0.2156m; 8.487 in.). The actuator width is chosen to span 10 degrees (0.1354m; 5.33 in.) of the cylinder circumference.

Table 5.3 Properties of the PSI-5H-S2 PZT actuator

Property	Value
d_{31} (m/V)	-274
Modulus of Elasticity (Pa)	6.2×10^{10}
Poisson's Ratio	0.31
K_{33}	3400
Initial Depolarization Field (V/m)	3.0×10^{5}
Density (kg/m^3)	7500

PZT actuation in bending (out of phase actuation) is not investigated for two reasons. It has been shown that PZT actuators exciting a cylinder with in phase actuation couple better with the interior acoustic field (lower order modes) than by using out of phase PZT actuation (Lefebvre, 1991). Also, since out of phase PZT actuation relies on the actuators being located away from the neutral axis of the shell, it is not practical because these actuators can not be placed on the exterior of the fairing skin.

5.2.5 PZT Actuator Location

Because the amount of excitation produced by the PZT actuator depends strongly on its position, it is necessary to place the actuator at a location that will couple well with the structural modes of interest. By placing the actuator at the middle of the cylinder, along its axial length, it will couple well with the odd axial modes (m = 1, 3, 5, 7, …). For the even modes, the placement is not as comprehensive because there is no spatial coincidence of the anti-nodes in the axial direction. The analysis will therefore investigate the response of the cylinder with an actuator placed at $l/2$ and $l/4$ for the cases described in sections 5.2.2 and 5.2.3.

5.2.6 Acoustic Field Point Location

This analysis is interested in the maximum acoustic levels a PZT actuator can generate within a cylinder. Because of the way the model is structured, it is difficult to get a mean or overall estimate of the interior acoustic field. It is therefore chosen to analyze a location that is representative of the maximum acoustic response within the cylinder. Because the acoustic mode shapes consist of cosine functions in the axial direction and align themselves circumferentially with the actuator, the maximum acoustic response is located near the end of the cylinder aligned with the PZT actuator. The field point in this analysis is chosen to be: $x = 0.99l$, $r = 0.99R_{ac}$, $\theta = 0^{\circ}$. This field point will essentially have the highest acoustic levels within the cylinder.

5.2.7 Summary of the Simulation Test Cases

In this analysis a variety of test cases are performed as described in sections 5.2.2, 5.2.3, and 5.2.5. Test Cases 1-7 are performed to investigate how the cylinder response changes as the stiffness and mass density are varied. The properties of the cylinder for each case are found in Table 5.2 and Appendix F. For each of these seven cases, the analysis is repeated for three different damping values. The entire analysis is also performed for the actuator located at $l/2$ and $l/4$. A total of 42 different test cases are performed and are summarized in Appendix G.

5.3 Results of the Simulations

The following section presents the results of the various simulations performed. The acoustic response of a pair of colocated PZT actuators is determined for 42 cases. The analysis is performed for a variety of cylinder parameters including, stiffness, mass, damping, and actuator location for an actuation frequency from 35 to 400 Hz. The current consumption of the actuator is also investigated.

5.3.1 Effect of Cylinder Stiffness and Mass Changes

The displacement response of the cylinder at $x = 0.4667l, \theta = 176^\circ$, actuated at $x = 0.5l, \theta = 0^\circ$, for cases 1-7 is shown in Fig. 5.2. Likewise the displacement response of the cylinder at $x = 0.2l, \theta = 176^\circ$, actuated at $x = 0.25l, \theta = 0^\circ$ is shown in Fig 5.3. The changes in parameters (stiffness and material density) do not have a large effect on the magnitude of the cylinder displacement response. The changes in magnitude appear to be frequency dependent and there is not one case that has a consistently larger response, compared to any other. The significant changes from case to case appear in the resonant frequencies of the cylinder. Likewise the interior acoustic response calculated at $x = 0.99l$, $r = 0.99R_{ac}$, $\theta = 0^\circ$ is not greatly affected from case to case as shown in Figs. 5.4 and 5.5, for cases 1a-7a and 1d-7d, actuated at $x = 0.5l, \theta = 0^\circ$ and $x = 0.25l, \theta = 0^\circ$, respectively. Because there is not a significant difference in the magnitude of the structural response (~ half an order of magnitude) or the internal acoustic response (~3 dB) between cases 1a-7a and 1d-7d, the remainder of the analysis concentrates on case 1a, 1d, 7a and 7d. These cases are chosen because they represent the extreme values of the seven cases.

It is important to note that for some of the cases (i.e. case 4d, at ~300 Hz) the acoustic response is well in excess of 130 dB. This level of actuation is undoubtedly in the non-linear range of the acoustic response. The reason the acoustic levels are so high for this particular frequency is explained by investigating the location of the structural and acoustic modes at ~300 Hz. The cylinder's structural (3,2) mode occurs at 299.11 Hz. Likewise the cylinder's acoustic (1,3,0) mode occur at 298.96 Hz. It is expected that the structural (3,2) mode would have the best coupling with the (1,3,0) acoustic mode compared to any of the other cylinder acoustic modes. In addition, these particular modes only differ in frequency by 0.15 Hz. For this reason the acoustic response is extremely high; however, it is doubtful that the actual level will reach that of what is predicted by the model.

5.3.2 Effect of Actuator Applied Voltage

As described in section 3.5, the cylinder internal pressure is proportional to the applied PZT actuator voltage. As the applied voltage increases linearly, the internal SPL varies logarithmically. If the applied voltage is doubled, the internal SPL will increase by ~6 dB. Likewise if the applied voltage is increased ten times, the internal SPL will increase by ~20 dB (see Figs. 3.9 and 3.10). Results of this effect are not presented, however this behavior has been verified for the overall cylinder model. This clearly is a limiting factor in using a PZT actuator to generate high internal SPLs.

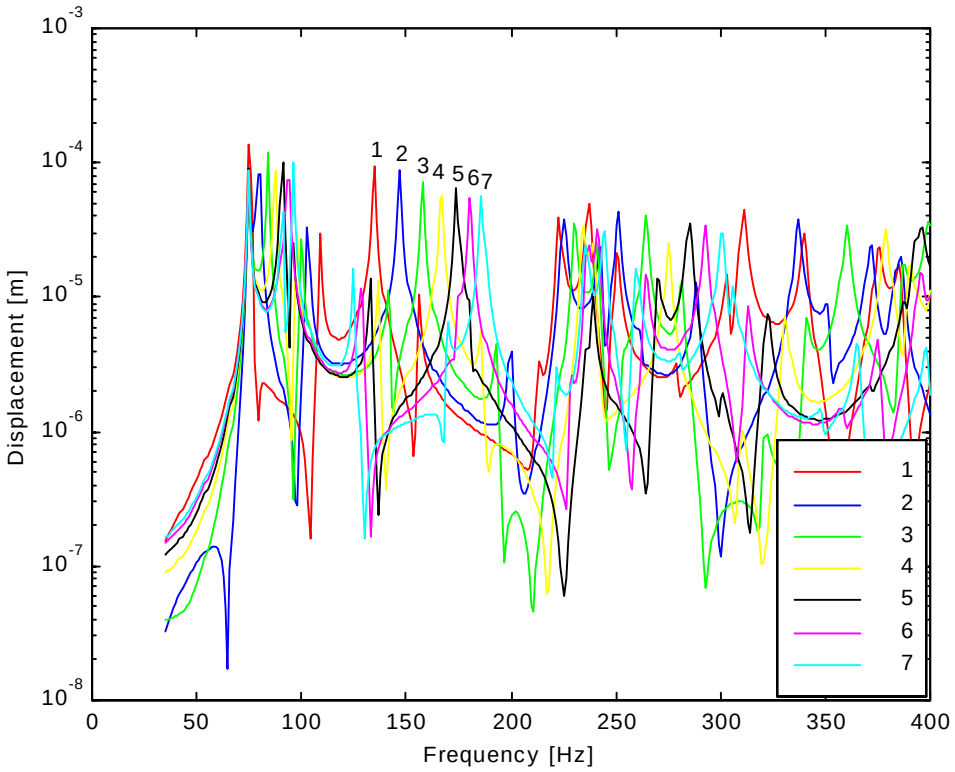

Figure 5.2 Cylinder displacement response actuated at $x = l/2, \eta = 0.007$, cases 1a-7a.

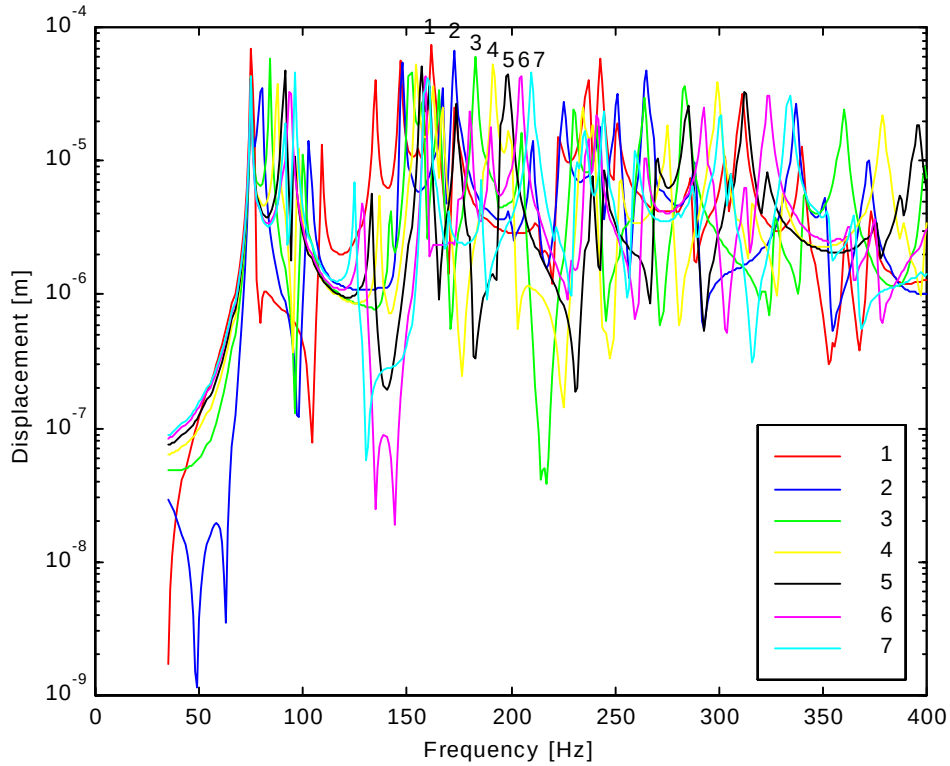

Figure 5.3 Cylinder displacement response actuated at $x = l/4, \eta = 0.007$, cases 1d-7d.

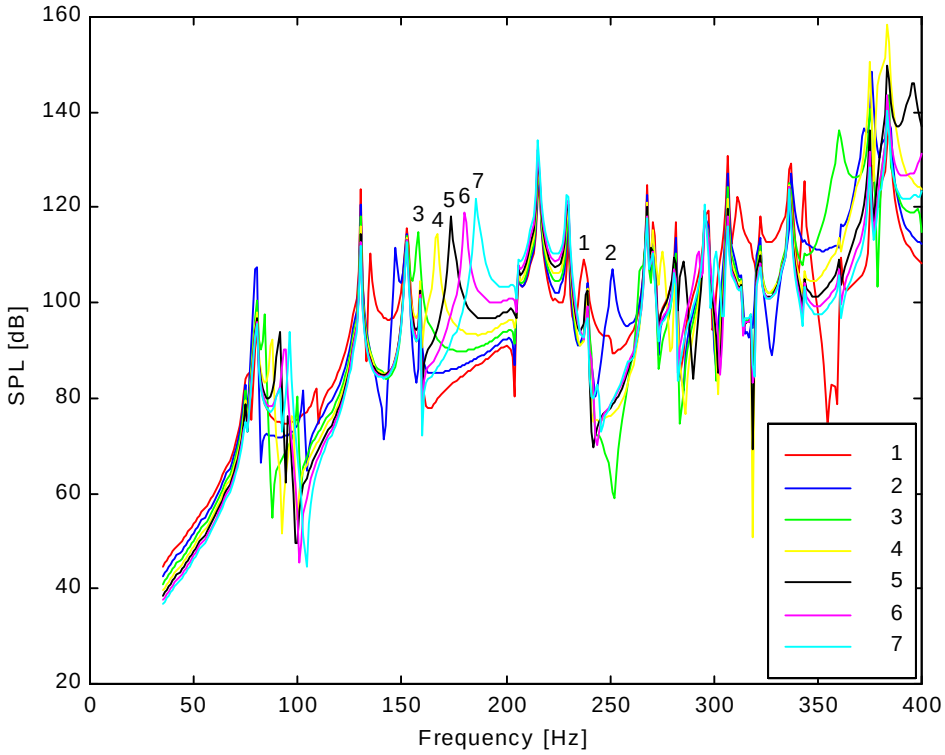

Figure 5.4 Pressure within the cylinder actuated at $x = l/2, \eta = 0.007$, cases 1a-7a.

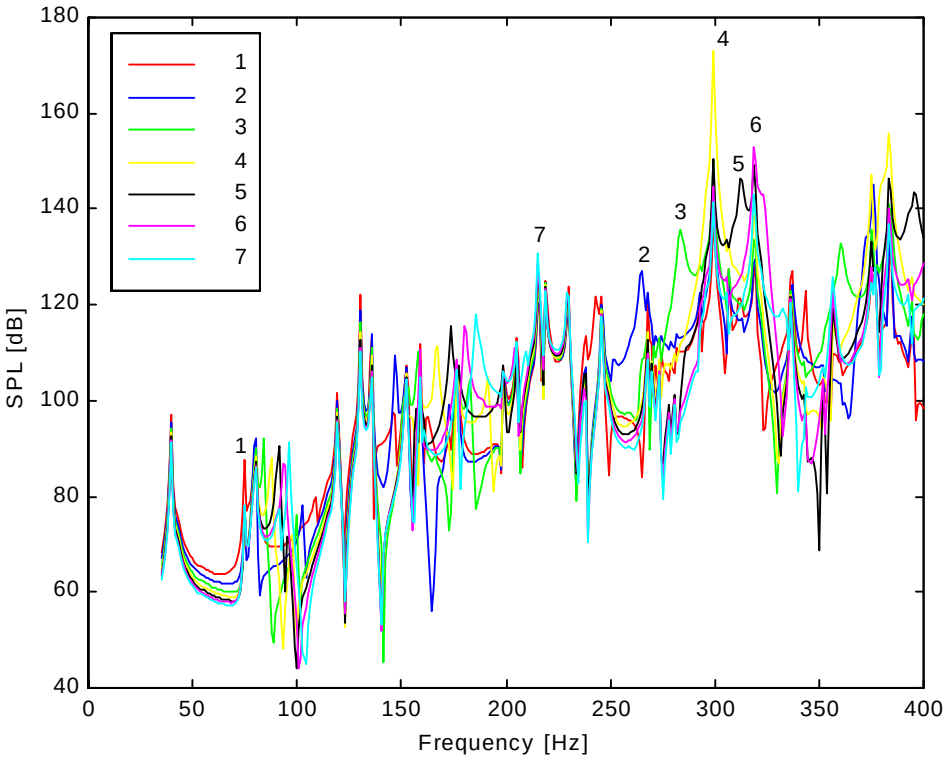

Figure 5.5 Pressure within the cylinder actuated at actuated at $x = l/4, \eta = 0.007$, cases 1d-7d.

5.3.3 Effect of Cylinder Damping Changes on the Acoustic Response

To investigate the effect of structural damping on the cylinder structural and acoustic response, case 1 and 7 are investigated for three different damping values: $\eta = 0.007$, $\eta = 0.0206$, and $\eta = 0.052$. The reason for choosing these particular values is described in section 5.2.3. The effect of hysteretic damping on the structural response of the cylinder is shown in Figs. 5.6 and 5.8 for case 1, actuated at $x = l/2$ and $x = l/4$, respectively. Clearly the effect of increased damping can be seen in the response magnitude. As the damping increases, the response of the cylinder is reduced near the resonant frequencies for the given PZT actuation. The response of the cylinder with the lowest damping is reduced approximately 16dB at the resonant frequencies, compared to the response of the cylinder having the highest damping.

Likewise, the effect of structural damping on the internal acoustic response of the cylinder is shown in Figs. 5.7 and 5.9 for case 1, actuated at $x = l/2$ and $x = l/4$, respectively. The significant reductions in the structural response due to increased damping do not produce a similar reduction in the acoustic SPLs for the cylinder. The acoustic levels at the acoustic resonant frequencies are essentially unaffected by the significant increase in structural damping. The acoustic levels at the structural resonant frequencies are mildly reduced due to the reduction in the structural response.

The results for the simulations described above are repeated for case 7 and are shown in Figs. 5.10-5.13. The results for case 7 are analogous to those produced for case 1. The general conclusion reached is that the interior acoustic response is dominated by the acoustic modes.

5.3.4 Implications to Active Structural Acoustic Control of Payload Fairings

As described in section 5.3.3, significant reductions in the structural response of the cylinder, at its structural resonant frequencies, provides little attenuation to the interior acoustic SPLs. This effect is caused for two reasons.

1. Away from the structural resonant frequencies of the cylinder, the structural response is not greatly affected by damping. Therefore, the spatial structural response of the cylinder is essentially the same regardless of damping and so the internal acoustic response is unaffected by the changes in the damping.

2. At the structural resonant frequencies, the damping significantly reduces the cylinder structural response. This does not necessarily equate to an equivalent decrease in the acoustic levels at that structural resonant frequency. Even though the dominant structural mode has been reduced at that frequency, it does not necessarily couple well with the dominant acoustic mode of the cylinder, at the structural resonant frequency.

Therefore, significant reductions in the overall interior acoustic levels will not be achieved if only the structural resonances are controlled. Since active structural control has traditionally strived to reduce the vibration levels of the structure or artificially increase the structure's damping, it is unlikely that these techniques will be effective to control fairing acoustics. These results are supported by an experiment performed by Glaese and Anderson on the STARS

fairing. In their experiment they found that high closed-loop damping ratios did not significantly reduce the acoustic field inside the fairing (Glaese and Anderson, 1999).

For modal restructuring (or rearrangement), the control system actively changes the magnitude and phase of the acoustically coupled structural modes. This reduces the overall acoustic response, but may cause the structural vibration amplitudes to increase. For an enclosed space, modal restructuring is effective because there are multiple structural modes, having similar magnitude, coupled into a single acoustic mode (Snyder and Hansen, 1994). One difficulty for modal restructuring is that the actuator must excite specific structural modes not at the resonant frequencies. This is a challenge since the structural impedance of the cylinder for a particular mode (modal shape) is very high away from the structural resonant frequency. The amount of actuation required for a PZT actuator to produce acoustic levels commensurate with the interior of a payload fairing is addressed in the next section.

5.3.5 Baseline Actuator Acoustic Authority

As was pointed out by Snyder and Hansen, "Heuristically, the best control will be achieved if the control sources are capable of "duplicating" the response of the system to the primary disturbance" (Snyder and Hansen, 1994). This implies that PZT actuators will be able to control fairing acoustics if they are able to generate a sound field equivalent to that created by the disturbance (~130 dB). By perusing Figs. 5.4 and 5.5 it can be seen that the baseline PZT actuator (described in section 5.2.4) used in this analysis will not be able to generate acoustic levels commensurate with that found within the fairing, particularly at the lower frequencies (below 200 Hz). Since the baseline actuator's applied voltage can not be increased, additional actuators are required in order to increase the response of the cylinder at some of the frequencies. The additional actuators will increase the overall current demands on the amplifier used. The next sections will address the amount of electrical current required for the baseline actuator. Following, the amount of additional current or number of actuators required to generate acoustic levels commensurate with the fairing will be determined.

It is interesting to note the trend in the acoustic levels shown in Figs. 5.4 and 5.5. The baseline actuator is clearly better at generating sound within the cylinder as the frequency increases. This implies that more actuators will be required to control the lower frequency acoustic modes than the higher frequency modes.

5.3.6 The Importance of Actuator Current Consumption

The design of electrical amplifiers usually has two properties that define their performance. One is the maximum deliverable voltage and the second is the maximum deliverable current. The product of these two properties defines the amplifier's deliverable power. Since the PZT actuator essentially acts like a capacitor, the applied actuator voltage and current are essentially ninety degrees out of phase. This implies that little or no power is being consumed by the actuator. This can be misleading from a practical point of view, implying that since the actuators consume very little real power, it is relatively easy to supply the necessary current and voltage. This is not necessarily true. Amplifiers that are capable of generating high voltages are generally readily available, however amplifiers that can produce a significant amount of current are not.

Usually electrical amplifiers are current limited. Typically, achieving more than an Ampere of current requires a specially designed amplifier. For linear amplifiers, the current delivered to the load is dissipated in the amplifier. Not only are high currents difficult to generate for linear amplifiers but the currents are dissipated internally producing heat within the amplifier. Another problem with high current levels is the size of the wire required to transmit the current. Every actuator requires two wires that can pass the required current. As the current levels become large, so will the size of the wire required to transmit the current. This may be a potential weight problem if many actuators are required for control. For active structural control of a fairing using PZT actuators, the most significant electrical limiting factor is the current consumption and not the required power or applied voltage.

5.3.7 Baseline Actuator Current Consumption

In this investigation the PZT actuator is modeled as a capacitor whose capacitance is given by:

$$C_a = K_{33}^T \varepsilon_o l_a R_a / t_a \tag{5.1}$$

where, $K_{33}^T, \varepsilon_o, l_a, R_a,$ and t_a represent the PZT dielectric constant (3400), permittivity of free space (8.85×10^{-12} F/m), actuator axial length (0.2156m; 8.487 in.), actuator circumferential length (0.1354m; 5.33 in.), and actuator thickness (0.762 mm; 0.030 in.), respectively. The electrical current passing through the actuator is therefore given by:

$$I_a = \imath \omega C_a V_a \tag{5.2}$$

where, $\imath, \omega, C_a,$ and V_a represent an imaginary number, the operating frequency, actuator capacitance (1.153×10^{-6}F), and applied voltage (228.6 V; 161.64 Vrms), respectively. For the baseline PZT actuator described in section 5.2.4, the current amplitude for harmonic excitation is shown in Fig. 5.14.

Because the actuator needs to control multiple frequencies, the current consumption will be investigated at significant acoustic frequencies, and then added utilizing the superposition principal.

5.3.8 Payload Fairing Acoustic Authority and Current Consumption

In order to obtain a measure of the current requirements for a PZT actuator (or actuators) to generate acoustic levels commensurate to a payload fairing environment, the system is analyzed in terms of 1/3 octave-band center frequencies (31.5, 40, 50, 63, 80, 100, 125, 160, 200, 250, 315, 400 Hz). This is done because the acoustic field within the fairing is usually represented in terms of the 1/3 octave-band frequencies. This section will investigate the acoustic authority and current consumption of the baseline actuator and also determine the number of actuators and current required to achieve acoustic levels commensurate to a payload fairing environment (~130 dB at each octave-band frequency).

For the baseline actuator (see section 5.2.4) operating at its maximum voltage, the current is determined at each frequency as shown in Fig. 5.15. Each of the bands can be thought of as a structural or acoustic mode that needs to be controlled. If the control signal consists of multiple frequencies, the electrical current from each of these frequencies will overlap at some point in time and result in a peak current. For the baseline PZT actuator, actuating at the 1/3 octave-band center frequencies, the peak current is approximately 3 Amperes.

The internal SPL for the cylinder at $x = 0.99l, r = 0.99R_{ac}, \theta = 0^{\circ}$ for actuation at $x = l/2$ and $x = l/4$ is shown in Figs. 5.16 and 5.17 for case 1 and 7, respectively ($\eta = 0.007$). From the acoustic frequency response it is possible to obtain the 1/3 octave-band representation of the acoustic field at that point. This is also shown in Figs. 5.15 and 5.17. In order to control the acoustic field within the fairing, the actuator needs to generate a SPL of ~130 dB across the spectrum. The maximum acoustic levels generated by the baseline actuator are sufficient at the higher frequency range but are not commensurate with the levels found in a typical fairing in the lower frequency range (below ~200 Hz). The additional SPL required at each 1/3 octave-band center frequency is shown in Figs. 5.18 and 5.19 for case 1 and 7, respectively. The additional SPL required becomes significant as the frequency is reduced. This indicates that the PZT actuator acoustic authority decreases as the frequency is reduced.

Knowing the additional SPL required, it is possible to determine the number of additional actuators needed to generate acoustic levels commensurate to that found in a typical fairing (~130 dB). The total number of actuators required varies as shown in Table 5.4 and can be expressed by Eq. 5.3.

$$\#\ of\ \ Actuators = 2^{\Delta L/6} \tag{5.3}$$

where, ΔL represents the additional required SPL for the cylinder. Equation 5.3 can be applied to the results obtained in Figs. 5.18 and 5.19 to determine the total number of actuators required to generate acoustic levels commensurate to the payload fairing environment (~130 dB). The number of actuators (or actuation) required, for case 1 and 7 is shown in Fig. 5.20. As the actuation frequency is reduced, the number of actuators required to generate higher SPLs increase to impractical values. Likewise, if the current amplitude is computed at each 1/3 octave-band center frequency, the result is shown in Fig. 5.21 and is compared to the baseline actuator current consumption. Below approximately 100 Hz, the current demands reach unfeasible levels.

5.4 Conclusions of the Simulations

The following conclusions can be made based on the simulations performed in this chapter:

1. The changes in parameters (stiffness and material density) from case to case do not have a large effect on the magnitude of the cylinder displacement response. The significant changes from case to case appear in the natural frequencies of the cylinder. Likewise the interior acoustic response calculated at $x = 0.99l$, $r = 0.99R_{ac}$, $\theta = 0^{\circ}$ is not greatly affected from case to case.

2. As the applied voltage increases linearly, the internal SPL varies logarithmically. If the applied voltage is doubled, the internal SPL will increase by ~6 dB. Likewise to achieve a ~20 dB increase in the internal sound field, it is necessary to increase the structural response ten times. This would require ten times the applied voltage or ten times the number of actuators. This clearly is a limiting factor in using a PZT actuator to generate high internal SPLs.

3. Significant reductions in the structural response due to increased damping do not show a similar reduction in the acoustic SPLs for the cylinder. The sound levels at the acoustic resonant frequencies are essentially unaffected by the significant increase in structural damping. The acoustic levels at the structural resonant frequencies are mildly reduced due to the reduction in the structural response.

4. The interior acoustic response is dominated by the acoustic modes and therefore, significant reductions in the overall interior acoustic levels will not be achieved if only the structural resonances are controlled.

5. The maximum acoustic levels generated by the baseline actuator are sufficient at the higher frequency range but are not commensurate with the levels found in a typical fairing in the lower frequency range (below ~200 Hz). Since the baseline actuator's applied voltage can not be increased, additional actuators are required in order to increase the response of the cylinder at some of the frequencies.

6. The baseline actuator is clearly better at generating sound within the cylinder as the frequency increases. This implies that more actuators will be required to control the lower frequency modes than the higher frequency modes.

7. As the actuation frequency is reduced, the number of actuators required to generate SPLs commensurate to the acoustic levels found in the fairing increase to impractical values. Below approximately 100 Hz, the current demands reach levels that are extremely difficult to achieve with a practical system.

It should be reiterated that the motion of the structure is assumed to be uncoupled with the internal acoustics, and so the structural-acoustic interaction (SAI) is not considered in this analysis. Including the SAI may produce different results and yield different conclusions.

Table 5.4 Increase in sound for a given actuation

Total # of Baseline Actuators	ΔL (dB)	Sound Generated (dB)
1	0	L_1
2	6	$L_1 + 6$
4	12	$L_1 + 12$
8	18	$L_1 + 18$
16	24	$L_1 + 24$
32	30	$L_1 + 30$
etc…	etc…	etc…

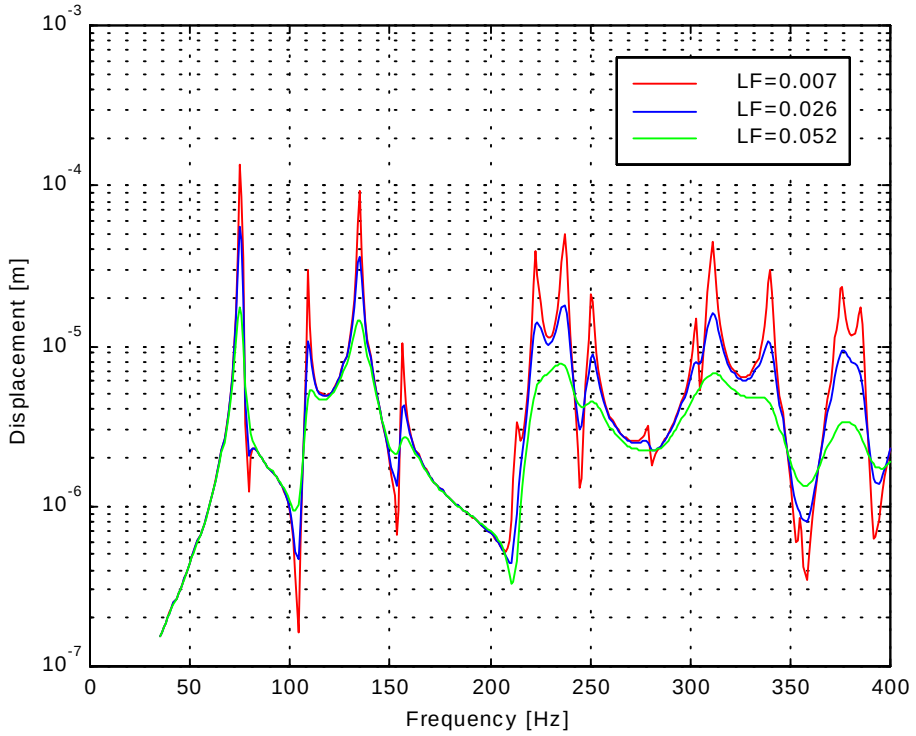

Figure 5.6 Cylinder displacement response actuated at $x = l/2$, case 1a, $\eta = 0.007$; case 1b, $\eta = 0.0206$; case 1c, $\eta = 0.052$.

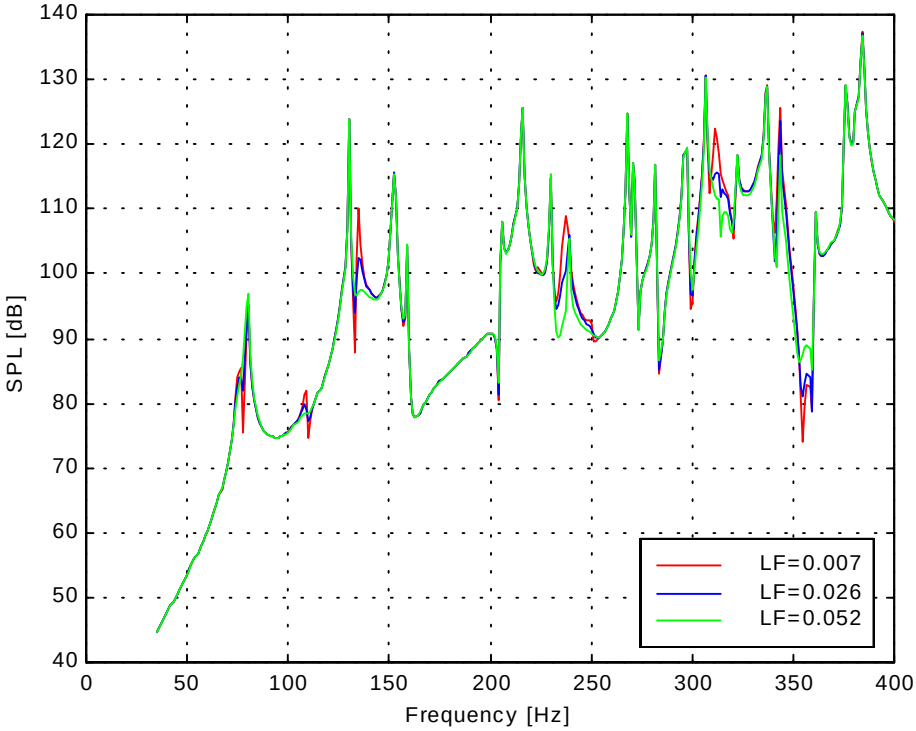

Figure 5.7 Cylinder SPL actuated at $x = l/2$, case 1a, $\eta = 0.007$; case 1b, $\eta = 0.0206$; case 1c, $\eta = 0.052$.

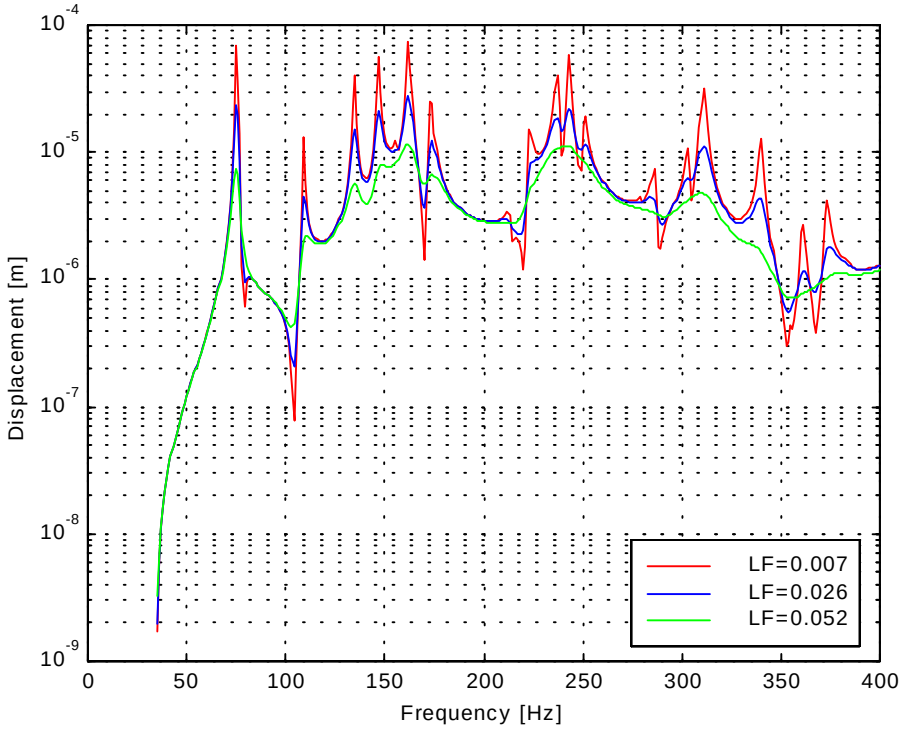

Figure 5.8 Cylinder displacement response actuated at $x = l/4$, case 1d, $\eta = 0.007$; case 1e, $\eta = 0.0206$; case 1f, $\eta = 0.052$.

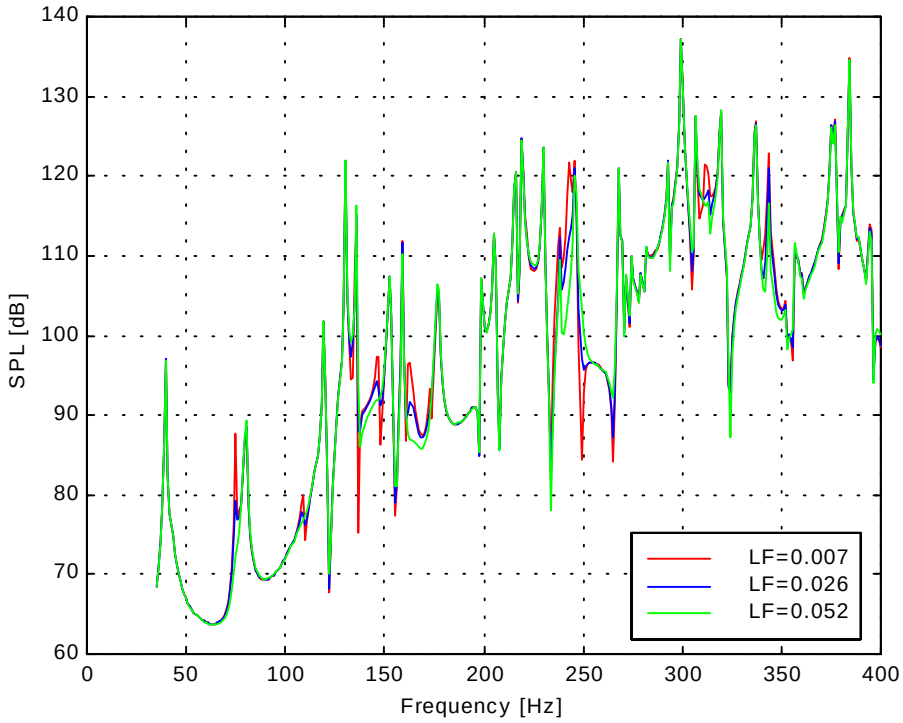

Figure 5.9 Cylinder SPL actuated at $x = l/4$, case 1d, $\eta = 0.007$; case 1e, $\eta = 0.0206$; case 1f, $\eta = 0.052$.

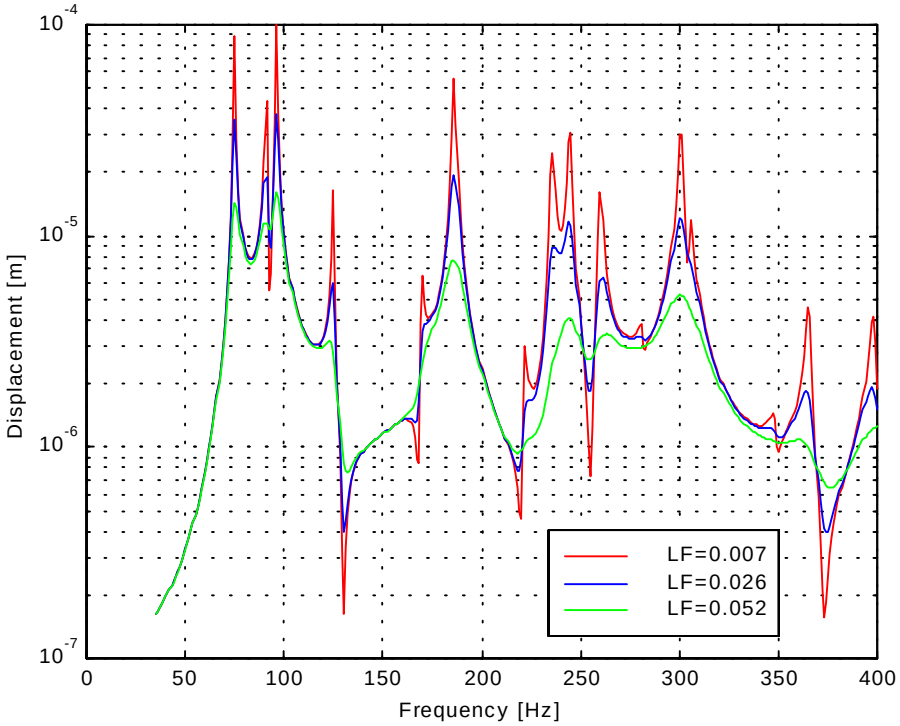

Figure 5.10 Cylinder displacement response actuated at $x = l/2$, case 7a, $\eta = 0.007$; case 7b, $\eta = 0.0206$; case 7c, $\eta = 0.052$.

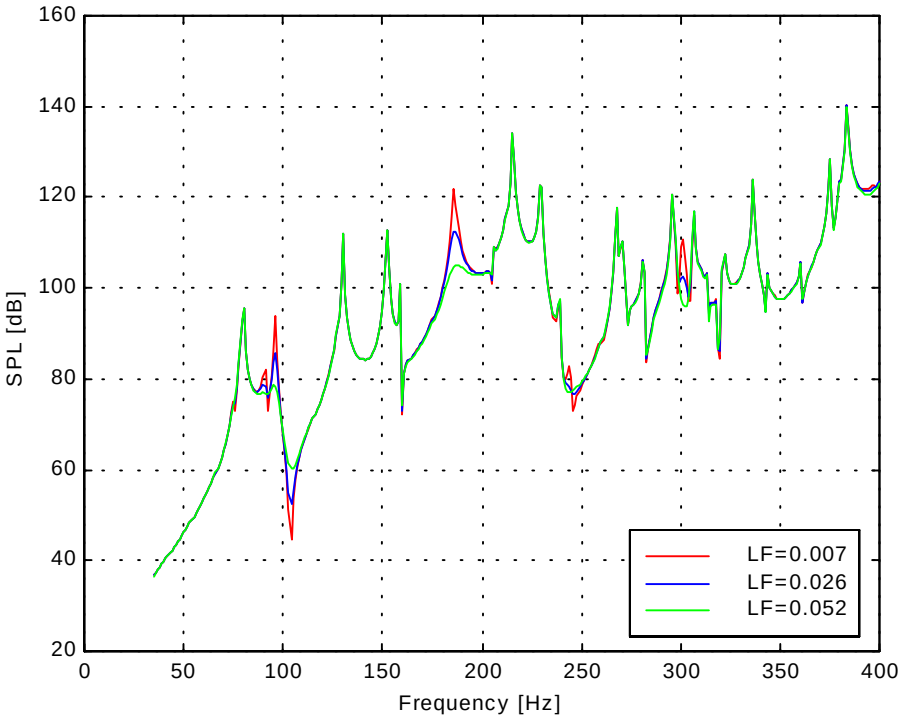

Figure 5.11 Cylinder SPL actuated at $x = l/2$, case 7a, $\eta = 0.007$; case 7b, $\eta = 0.0206$; case 7c, $\eta = 0.052$.

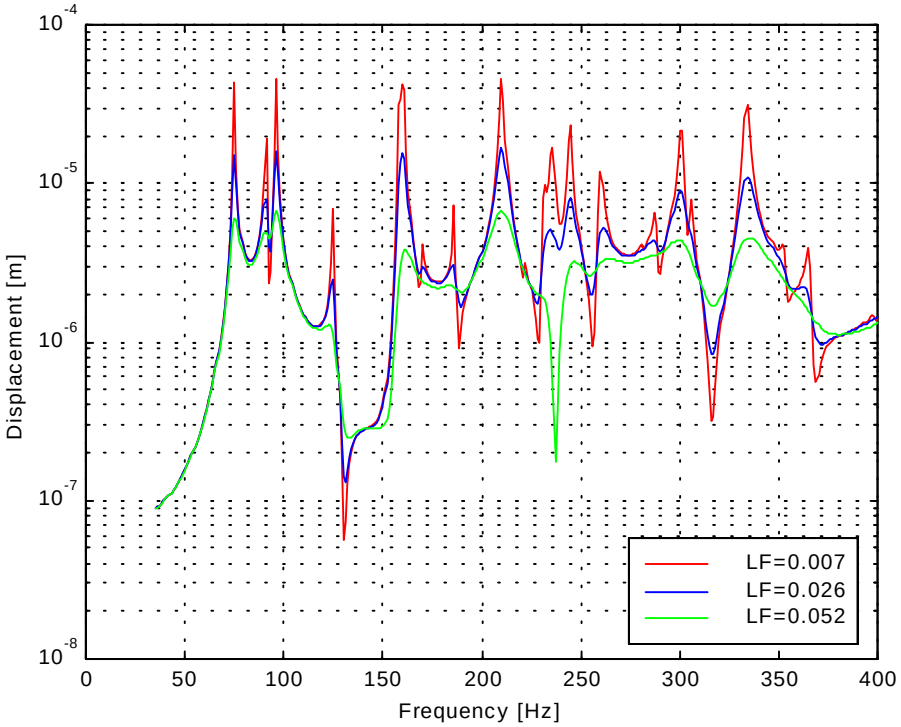

Figure 5.12 Cylinder displacement response actuated at $x = l/4$, case 7d, $\eta = 0.007$; case 7e, $\eta = 0.0206$; case 7f, $\eta = 0.052$.

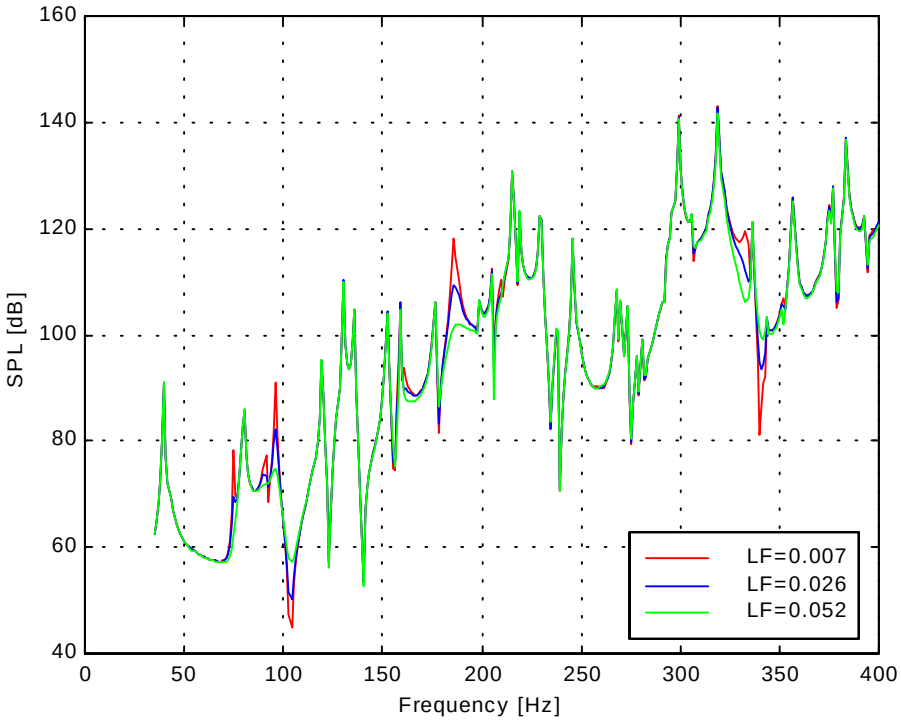

Figure 5.13 Cylinder SPL actuated at $x = l/4$, case 7d, $\eta = 0.007$; case 7e, $\eta = 0.0206$; case 7f, $\eta = 0.052$.

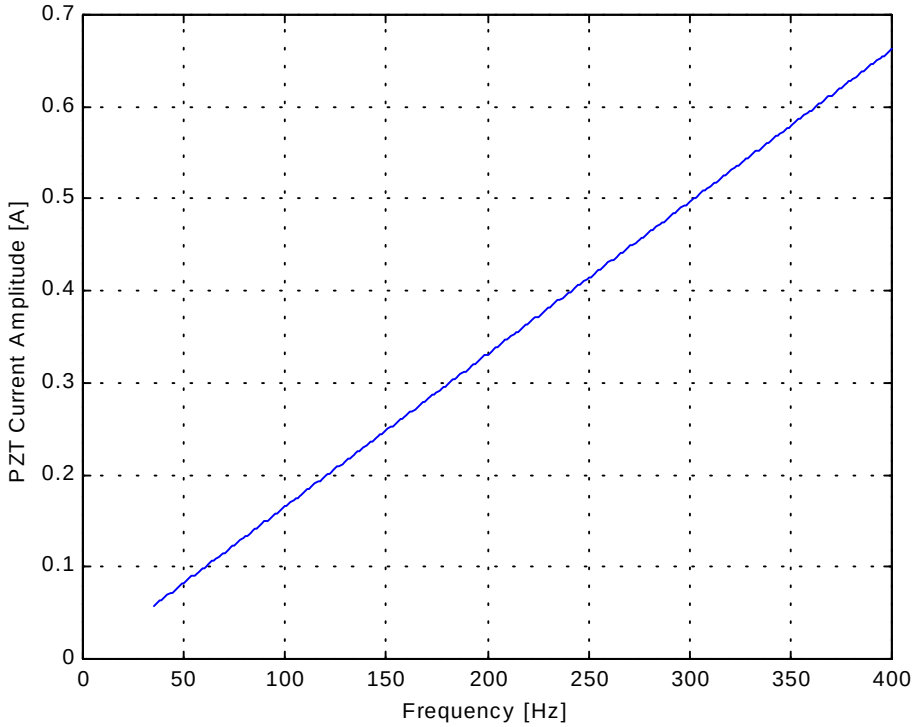

Figure 5.14 Baseline PZT actuator current draw for harmonic excitation.

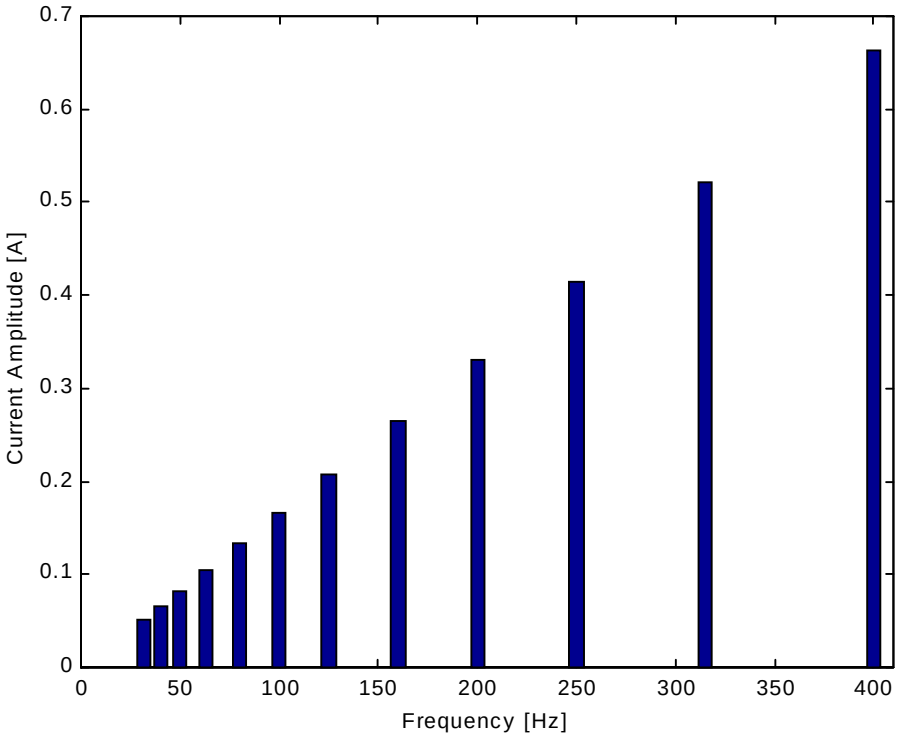

Figure 5.15 Baseline PZT actuator current at the 1/3 octave-band center frequencies.

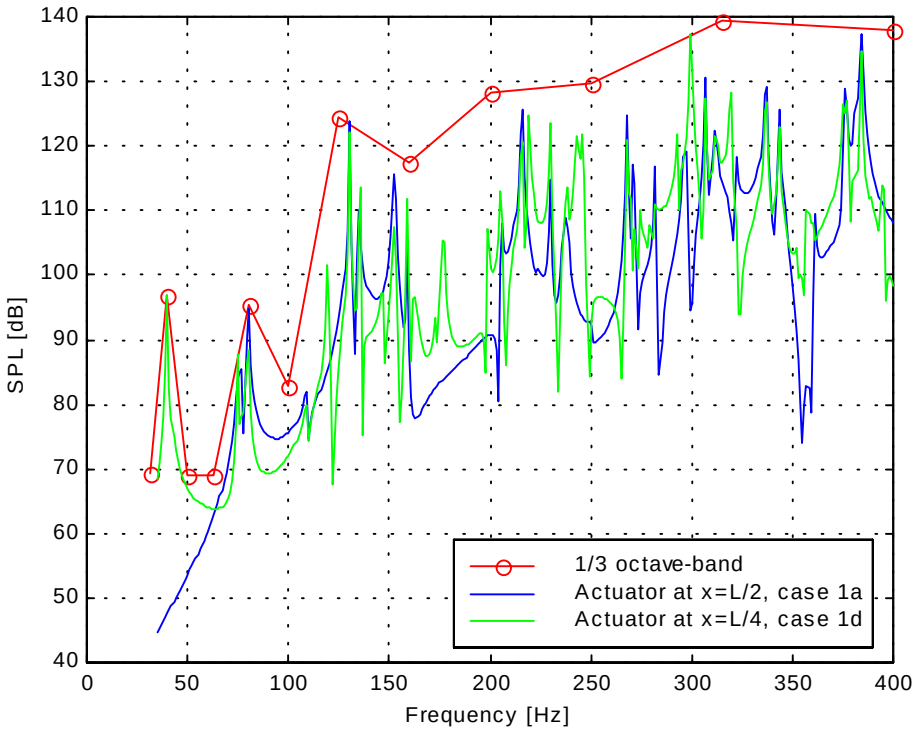

Figure 5.16 Cylinder internal acoustic levels and 1/3 octave-band representation for case1.

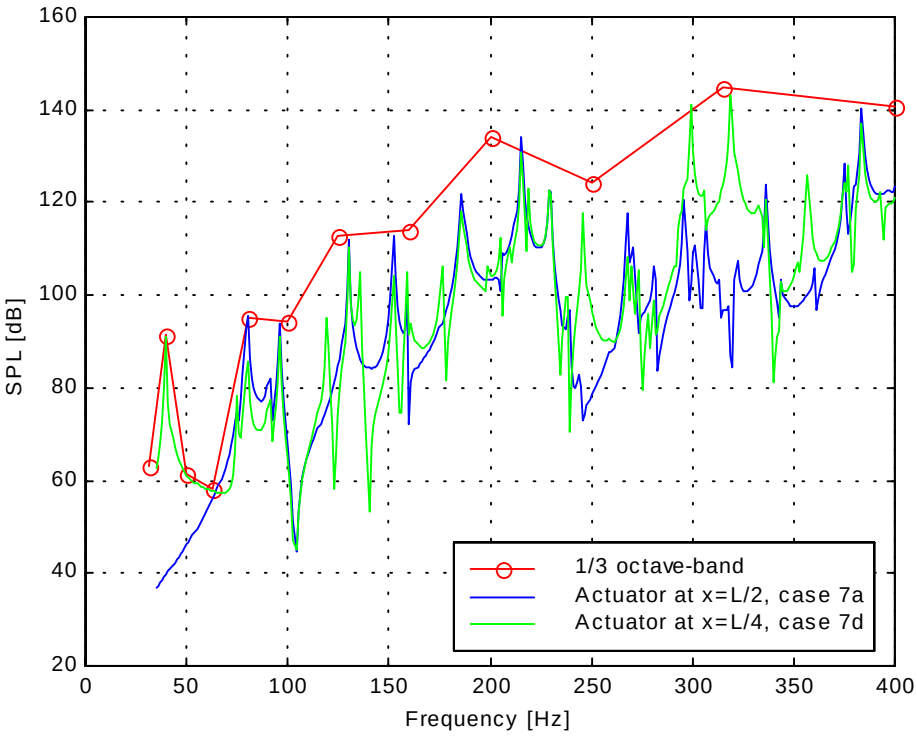

Figure 5.17 Cylinder internal acoustic levels and 1/3 octave-band representation for case7.

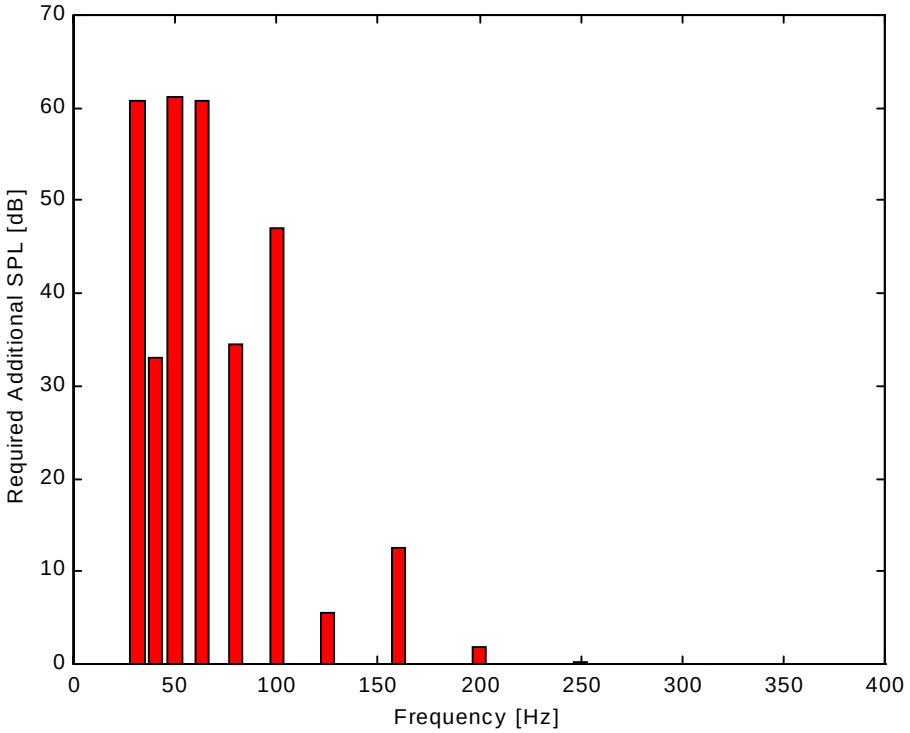

Figure 5.18 Additional SPL required to achieve 130 dB, case1.

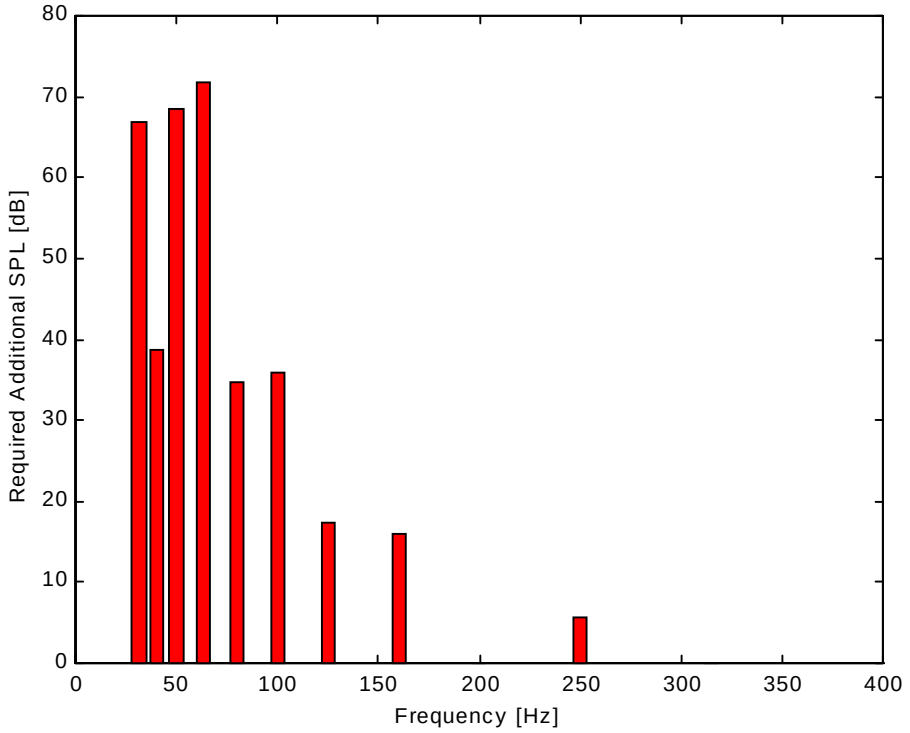

Figure 5.19 Additional SPL required to achieve 130 dB, case7.

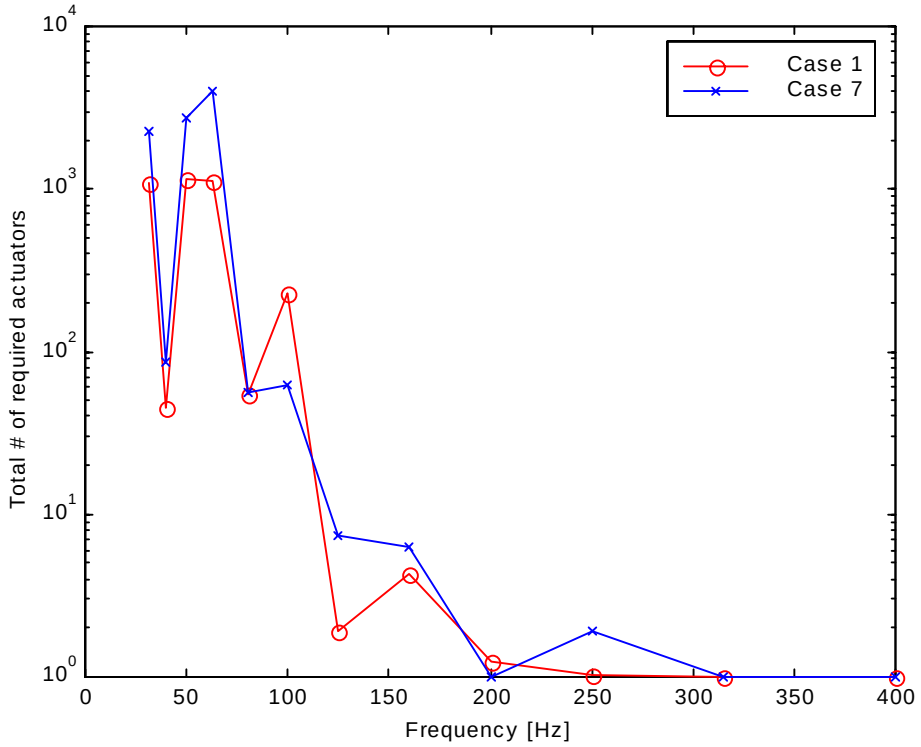

Figure 5.20 Required number of baseline PZT actuators to achieve 130 dB.

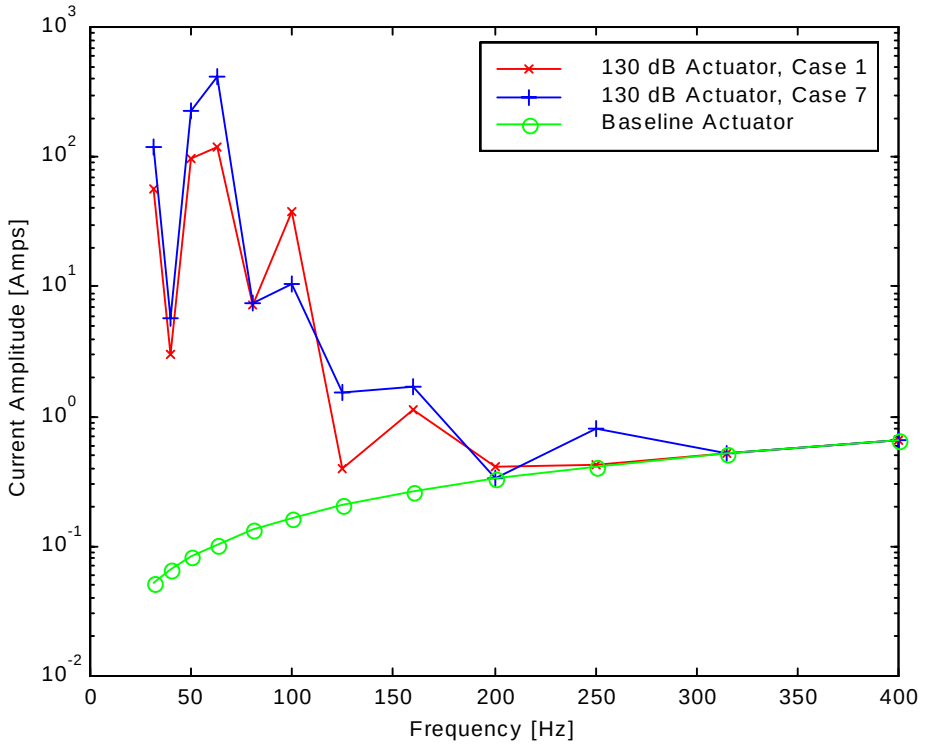

Figure 5.21 Required current amplitude to achieve 130 dB.